



Heterogeneous & Homogeneous & Bio- & Nano-

CHEM **CAT** CHEM

CATALYSIS

Accepted Article

Title: On the mechanism of the Ruthenium-catalyzed β -methylation of alcohols with methanol

Authors: Markus Hoelscher, Walter Leitner, Marc Schmitz, and Akash Kaithal

This manuscript has been accepted after peer review and appears as an Accepted Article online prior to editing, proofing, and formal publication of the final Version of Record (VoR). This work is currently citable by using the Digital Object Identifier (DOI) given below. The VoR will be published online in Early View as soon as possible and may be different to this Accepted Article as a result of editing. Readers should obtain the VoR from the journal website shown below when it is published to ensure accuracy of information. The authors are responsible for the content of this Accepted Article.

To be cited as: *ChemCatChem* 10.1002/cctc.201901871

Link to VoR: <http://dx.doi.org/10.1002/cctc.201901871>

WILEY-VCH

www.chemcatchem.org

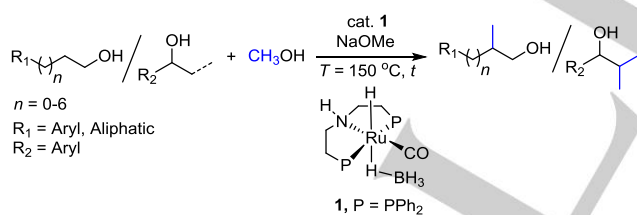


On the mechanism of the Ruthenium-catalyzed β -methylation of alcohols with methanol

Akash Kaithal,^[a] Marc Schmitz,^[a] Markus Hölscher*^[a] and Walter Leitner*^[a,b]

Abstract: Selective β -methylation of alcohols with methanol has been recently described using a catalytic system comprising the ruthenium pincer complex $[\text{RuH}(\text{CO})(\text{BH}_4)(\text{HN}(\text{C}_2\text{H}_4\text{PPh}_2)_2)]$ (Ru-MACHO-BH) **1** and alcoholate bases as co-catalysts.^[1] Here we present a detailed mechanistic analysis for the mono-methylation of 1-phenyl-propane-1-ol **2a** as prototypical example. Several experimentally observed intermediates were localized as stable minima on the DFT-derived energy surface of the entire reaction network. The ruthenium complex $[\text{Ru}(\text{H})_2(\text{CO})(\text{HN}(\text{C}_2\text{H}_4\text{PPh}_2)_2)]$ **I** was inferred as the active species catalyzing the dehydrogenation/re-hydrogenation of substrates and intermediates („hydrogen borrowing“). The hydrogen-bonded alcohol adduct of this complex was identified as the lowest lying intermediate (TDI). The C-C bond formation results from a base-catalyzed aldol reaction comprising the transition state with the highest energy (TDTS). Experimentally determined Gibbs free activation barriers of 26.1 kcal/mol and 26.0 kcal/mol in methanol and toluene as solvents, respectively, are reflected well by the computed energy span of the complex reaction network (29.2 kcal/mol).

Catalytic methods for the introduction of methyl groups into organic substrates using methanol as C1 building block offer attractive synthetic pathways in line with the principles of Green Chemistry. In particular the synthesis of methyl branches in aliphatic carbon chains using methanol remains a significant challenge, however.^[2] Most recently we showed that ruthenium pincer complex $[\text{RuH}(\text{CO})(\text{BH}_4)(\text{HN}(\text{C}_2\text{H}_4\text{PPh}_2)_2)]$ (Ru-MACHO-BH) **1** is a versatile pre-catalyst for this reaction.^[1]

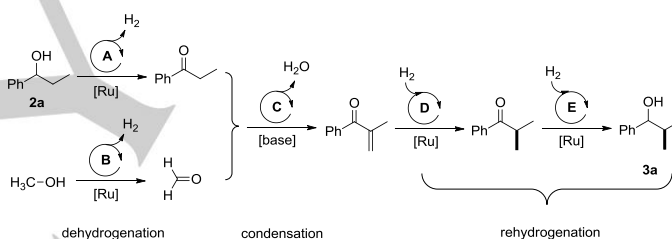


Scheme 1. β -Methylation of secondary and primary alcohols with pre-catalyst **1** using methanol as C1 source.^[1]

For a broad range of primary and secondary alcohols as substrates, the methyl group is introduced selectively in

β -position providing the branched products in good to very high yields with water as the only byproduct (Scheme1). The synthetic methodology has been transferred and largely extended by the use of Mn(I)-MACHO complex most recently.^[3] In this work we present a mechanistic analysis of this transformation with the original ruthenium catalyst based on experimentally and theoretically compiled data.

From the results of the synthetic studies, we postulated a working hypothesis for the catalytic process exemplified in Scheme 2 for the mono-methylation of 1-phenyl-propane-1-ol **2a** to 1-phenyl-2-methyl-propane-1-ol **3a**. The overall transformation involves five individual cycles A-E forming a complex reaction network. Initially both alcohol and methanol are dehydrogenated by the transition metal catalyst to form ketone and formaldehyde, respectively.^[4] Subsequently, a base-catalysed aldol condensation generates the C-C bond^[5] and finally the unsaturated intermediate is step-wise re-hydrogenated at the ruthenium catalyst.



Scheme 2. Postulated reaction network based on experimental data of the mono-methylation of **2a** with methanol proceeding via subcycles A-E.^[1]

The involvement of the de- and re-hydrogenation cycles is corroborated with a series of control experiments summarized in scheme 3. 1-phenyl-propane-1-ol **2a** reacts with $^{13}\text{C}_3\text{H}_7\text{OH}$ to the mono-methylated product containing the ^{13}C -label exclusively in the new methyl branch (Scheme 3, entry a). A similar experiment with CD_3OD starting from 1-phenylethanol **2b** as the substrate shows the incorporation of deuterium at the methyl groups as well as in the α - and β -position of the alcohol moiety of the product (Scheme 3, entry b). Implying the carbonyl compounds as intermediates is confirmed by catalytic reaction of acetophenone **2a'** with an excess of methanol that leads to the expected methylated products (Scheme 3, entry c). *Vice versa*, the use of trioxane as formaldehyde source results in mono- and dimethylation of 1-phenylethanol under H_2 atmosphere (Scheme 3, entry d).

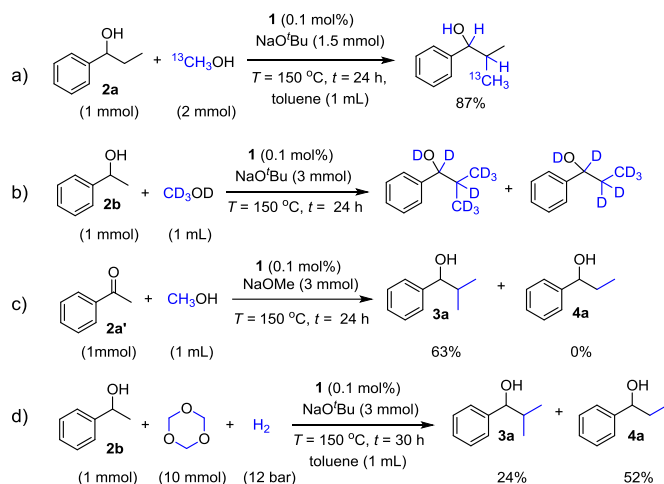
In order to get insight into the de-hydrogenation cycles A and B, the reaction of complex **1** with 2-phenylethanol **2c** and methanol was studied by multinuclear NMR spectroscopy (Scheme 4). Treatment of **1** with 1 equiv. of 2-phenylethanol **2c** in $[\text{D}_8]$ -toluene at 100°C revealed formation of the alcoholate complex **4** exhibiting a hydride signal in the ^1H NMR spectrum at -16.92 ppm (t, $J = 18$ Hz). Formation of aldehyde **5** and H_2 was confirmed by their characteristic signals at 9.24 (t, $J = 3$ Hz) and 4.50 ppm, respectively. Upon reacting **1** with methanol under similar conditions, the analogous methanolate complex **6** was

[a] A. Kaithal, Dr. M. Schmitz, Dr. M. Hölscher, Prof. Dr. W. Leitner
Institut für Technische und Makromolekulare Chemie
RWTH Aachen University
Worringer Weg 2, 52074 Aachen
E-mail: hoelscher@itm.rwth-aachen.de

[b] Prof. Dr. W. Leitner
Max Planck Institute for Chemical Energy Conversion
Stiftstraße 34-36, 45470 Mülheim/Ruhr
E-mail: walter.leitner@cec.mpg.de

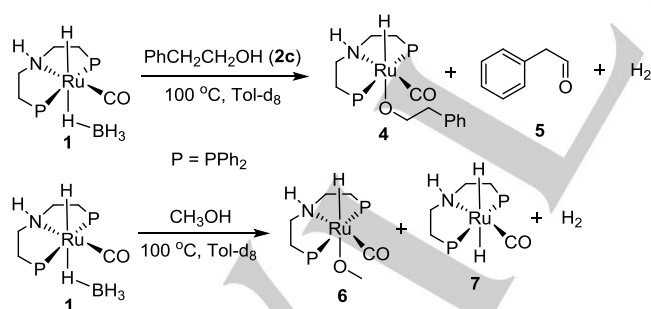
Supporting information for this article is given via a link at the end of the document.

formed. In addition, the resonance for the known di-hydride complex **7** was observed at -6.14 ppm (t , $J = 18$ Hz) by ^1H NMR. Importantly, the characteristic signal of dissolved H_2 is observed in both cases. These data clearly demonstrate the ability of pre-catalyst **1** for the dehydrogenation of alcohol substrates.



Scheme 3. Control experiments to probe the catalytic network shown in Scheme 3: Reactions (a, b) prove the incorporation of methanol and indicate extensive H/D scrambling during de-/re-hydrogenation. The methylation of acetophenone (c) supports that the alcohol substrate is initially dehydrogenated. Methylation with trioxane (d) as an alternative formaldehyde source in presence of H_2 supports the dehydrogenation of methanol.

The ruthenium dihydride complex $[\text{Ru}(\text{H})_2(\text{CO})(\text{HN}(\text{C}_2\text{H}_4\text{PPh}_2)_2)]$ can be plausibly inferred as common organometallic intermediate to explain the observed reactivity outlined in Scheme 4. The formation of **I** upon dissociation of BH_3 from **1** was described already by other groups.^[6] Formal addition of the OH groups from the alcohol substrates across the N-H and Ru-hydride bond leads to alcoholate complexes **4** and **6**, respectively.^[4b, 7]



Scheme 4. Reactions of pre-catalyst **1** with alcohol substrates monitored by multinuclear NMR spectroscopy (see SI for full details and representative spectra).

Based on these results we investigated by means of DFT computations (B97-D3BJ/def2-TZVP), if plausible reaction pathways leading to a closed catalytic cycle of the entire

reaction network can be mapped out for the methylation of 1-phenylpropan-1-ol **2a** with methanol as substrate using **I** as the catalytically active species (Figure 1). The geometries of the local minima and transition states were optimized in condensed phase (implicit treatment of the solvent methanol using the SMD model). If not mentioned otherwise we refer to Gibbs free energies in the following discussion. As the computed reaction pathways comprise all intermediates and transition states its analysis requires their connection in a sequential order as shown in Figure 1. The discussion below follows the definition of subcycles A to E as defined in Scheme 2 for clarity. In subcycles A and B the de-hydrogenation of the substrate alcohol **2a** and methanol are described, while subcycle C deals with the aldol condensation in which the C-C bond of the product is formed. Subcycles D and E refer to the re-hydrogenation to the final product **3a**.

The initial step in subcycle A is the formation of a hydrogen bridge between substrate **2a** and the NH-proton of the pincer ligand of **I** (**II**). The proton of the OH group of **2a** is oriented towards one of the two hydride centres at the ruthenium centre. The first chemical transformation consists of the OH proton transfer to the hydride, which leads to the formation of a non-classically bonded H_2 molecule at the metal centre (**TSII-III**; 12.0 kcal/mol). Next, the H_2 molecule dissociates from the complex (**IV**) and the hydrogen bonded alcoholate reorients and forms a Ru-O-bond leading to the endergonic formation of compound **V**. Dissociation of the alcoholate with concomitant reorientation enables a hydride transfer from the alcoholate carbon atom to the ruthenium centre (**TSV-I'**; 6.9 kcal/mol) and ketone **A** is eliminated from the complex while **I** is regenerated (**I'**). With regard to the energy of the reference point, subcycle A can be regarded overall as almost thermo neutral (reaction from **I** to **I'**), with barriers being so low that the subcycle can proceed at room temperature at high rates.

In subcycle B methanol is dehydrogenated to formaldehyde (**B**) and H_2 following the same principal reactions steps as outlined for subcycle A. Again, the barrier heights are not very pronounced and should enable a facile reaction at moderately elevated temperatures. This is a key enabling factor for the catalyst in this transformation, as the dehydrogenation of methanol is perceived often as particularly challenging. As a result of subcycles A and B active species **I''** is present in the reaction mixture as well as ketone **A**, formaldehyde **B** and two H_2 molecules, in accord with the experimental observations. The reaction system at this stage resides at a height of 13.3 kcal/mol. In principle alternative mechanistic pathways would be possible which rely on the concerted cleavage of a proton and a hydride from **I'** and its successors, **I''** and **I'''** (vide infra). Such a channel is indicated in Figure 1 showing complex **X**. However, the barrier from **I'** to **X** is fairly high and puts **TSI'-X** at an energy of 40.9 kcal/mol on the hyper surface, indicating that the system will not travel via this transition state.

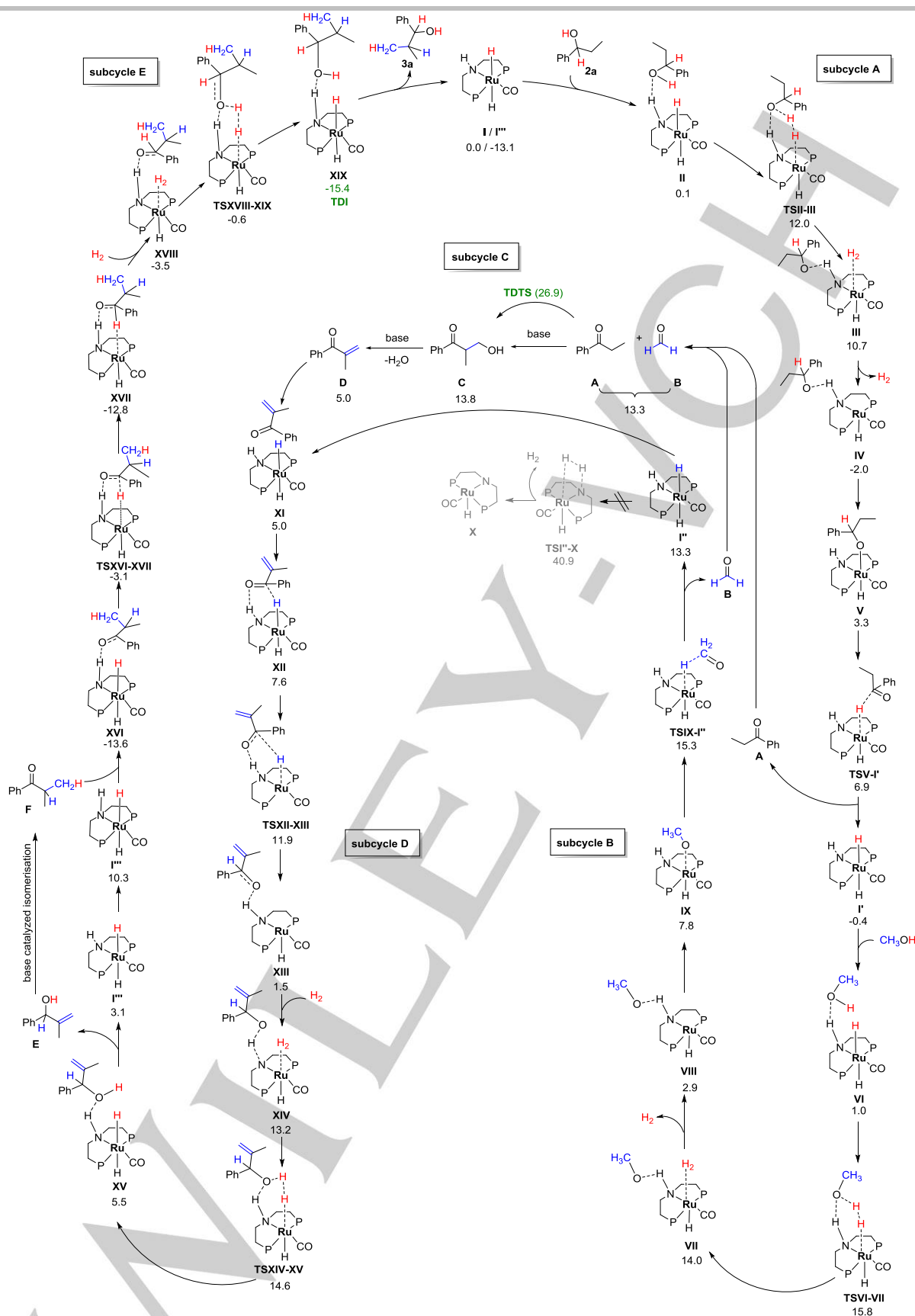


Figure 1. Computed catalytic subcycles A-E (relative Gibbs free energies ΔG in kcal/mol) with turn over determining intermediate (TDI)[8] and turn over determining transition state (TDTS; green). In subcycles A and B substrate and methanol, respectively, are dehydrogenated, while in subcycle C the C-C bond formation occurs base catalyzed with concomitant generation of H₂O. Subcycle C (aldol condensation) is described in the SI in detail. In subcycles D and E compounds D and E/F are rehydrogenated, respectively closing the overall catalytic cycle.

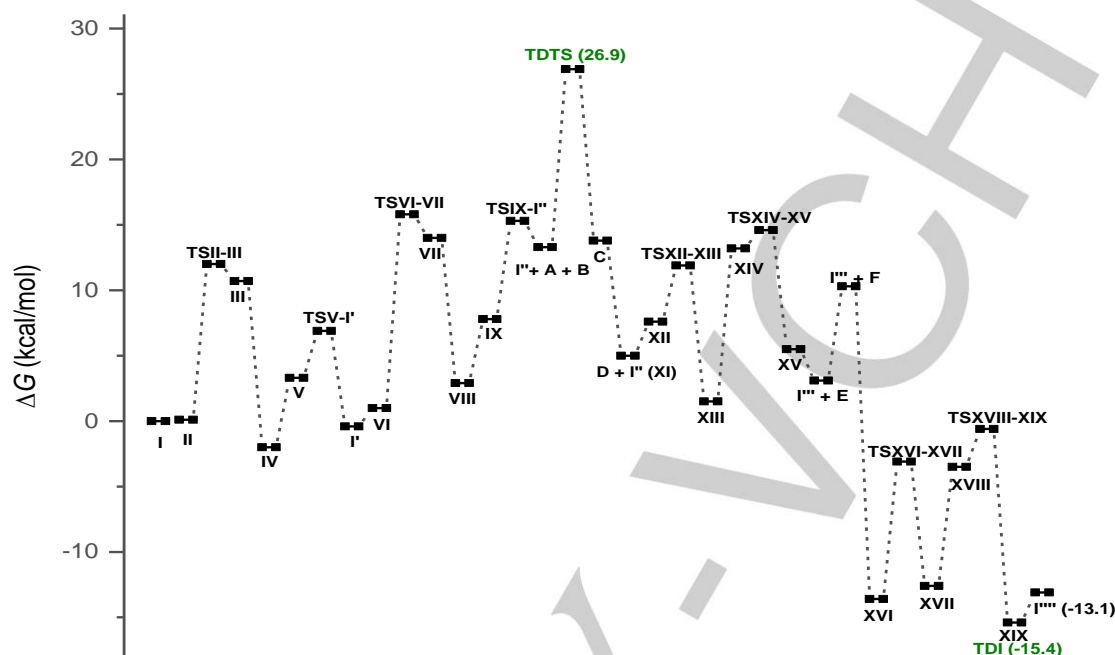


Figure 2. Energy profile for the catalytic cycle as shown in Figure 1 showing TDI and TDS green. The TDS is part of subcycle C (aldol condensation) which is described in detail in Figure 3 and in the SI.

As is shown abbreviated in Figure 1 the C-C bond formation is a purely base catalyzed event taking compounds A and B via C to D. For the sake of clarity these steps are shown in more detail in Figure 3.

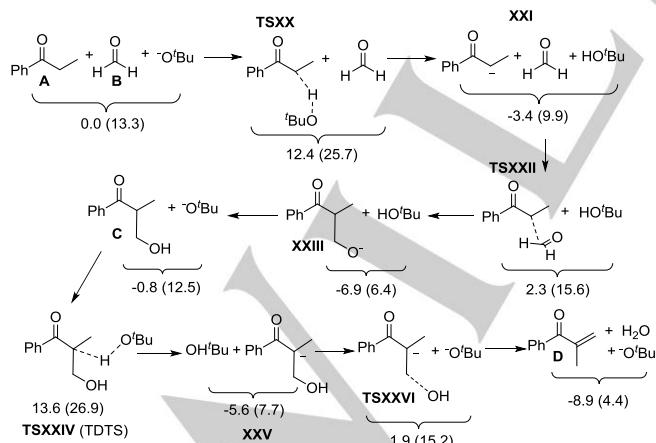


Figure 3. B97D3-BJ/def2-TZVPD(SMD) optimized structures of the aldol condensation of subcycle C with relative Gibbs free energies (kcal/mol). Values in parenthesis are derived by adding 13.3 kcal/mol to the def2-TZVPD derived values to obtain an estimate of the energy position of the compounds

on the def2-TZVP hyper surface. Further details on the derived energies are given in the SI.

Subcycle C comprises a classical base catalyzed aldol condensation, in which the unsaturated ketone D and one equivalent of H₂O are formed. Most notably, however, this subcycle contains the rate determining transition state (TDS),^[8] the energy of which is represented for clarity in Figure 1 over the bow leading from A/B to intermediate C. As the anionic base ^tBuO⁻ is an active reagent in subcycle C, the geometries of the local minima and transition states were optimized using the def2-TZVPD basis set (in contrast to the def2-TZVP basis set used in subcycles A, B, D and E). This larger basis set includes diffuse functions which are advantageous for the description of anionic systems to arrive at energies of a sufficiently high quality for quantitative evaluations of the cycle. As energies computed with different basis sets cannot be compared directly we have optimized the most important stationary points of subcycle C independently using both basis sets and found no significant differences in energies. Further details on how to include the def2-TZVPD derived energies into the def2-TZVP derived energy profile is given in detail in the SI.

Subcycle D starts with the formation of a loosely coordinated ensemble of I'' and D (XI), which subsequently establishes a N-H...O hydrogen bond and a C-H...Ru interaction (XII). In the subsequent reaction step the hydride centre is transferred from

the metal centre to the carbonyl C atom of D (**XIII**) and then one of the H₂ molecules generated earlier in the reaction takes part in the first re-hydrogenation step (**XIV**) leading the reaction to **XV**. After dissociation of the unsaturated alcohol **E** from **XV** the active species is regenerated (I^{III}) while **E** isomerizes base catalyzed to ketone **F**,^[9] which associates to I^{III} and forms **XVI**. It should be noted that in principle the olefinic C-C-double bond of **E** could also be hydrogenated. However, experimentally **E** was not observed in the reaction mixture, while **F** was detected in significant amounts. It is therefore plausible to assume a fast isomerization of **E** and the subsequent hydrogenation of the C=O bond of **F** is favored. In subcycle E the keto group of **F** is hydrogenated following the same principle steps as in subcycle D.

With regard to the overall Gibbs free activation energy it is worthwhile noting that all single barriers are either low or of moderate height throughout the whole catalytic cycle and therefore can easily be overcome. However, it was observed experimentally that reasonable reaction rates can be achieved only at temperatures of around 150°C. The requirement of high reaction temperatures results from the fact that the TDTS (C-C bond forming step in subcycle C; **TSXXIV**, see SI) lies at 26.9 kcal/mol on the hyper surface while the TDI (**XIX**, subcycle E) has a pronounced stability at -15.4 kcal/mol. Accordingly, the overall Gibbs free activation energy (i.e. the energy span) is calculated as the sum of the absolute values of TDI and TDTS (15.4 + 26.9 kcal/mol) subtracted by the Gibbs free reaction energy ΔG_r (-13.1 kcal/mol) amounting to a value of ΔG[#] = 29.2 kcal/mol. This value compares reasonably well with the experimentally determined value of ΔG[#] = 26.1 +/- 0.5 kcal/mol estimated from conversion/time-experiments and in this way supports the derived mechanism.^[10]

Conclusions

In summary, the various reaction pathways of a complete reaction network of a Guerbet-type C-C methylation using methanol as C1 source has been analyzed computationally using density functional theory. Based on experimental evidence for organometallic and organic intermediates involved in the individual cycles, the frequently postulated combination of de-hydrogenation, aldol coupling, and re-hydrogenation was evaluated for the specific case of the Ru-MACHO-BH catalyst. It was found that the metal catalyzed de- and re-hydrogenation cycles are characterized by moderate barriers in the range of around ca. 10-15 kcal/mol. Also the base catalyzed C-C bond formation has only a moderate barrier of 13.6 kcal/mol, but involves the highest transition state on the energy surface at 26.9 kcal/mol relative to the reference point. Together with the high stability of the dihydride complexes in presence of the alcohol/ketone substrates (particularly **XVI**, **XVII** and **XI**), this results in a significant energy span of 29.2 kcal/mol that correlates well with the observed high reaction temperatures.

The insight obtained from this study may provide valuable information for the design of effective catalysts for this general reaction type. It is generally assumed that the activity and hence the transition states of the metal catalyst dehydrogenation are limiting factors for the rate of product formation. However, the present analysis indicates that the intermediate adducts with substrates in the re-hydrogenation should be targeted with the

aim to destabilize them in order to minimize the overall activation barrier/energy span that is ultimately determining the apparent turnover frequency. Like in a clockwork, it is the wheel that is hardest to turn that defines the rate of the overall movement.

Computational and Experimental Details

The DFT calculations and all experiments are described in detail in the SI. Cartesian coordinates of the compounds computed are provided by the authors upon request.

Acknowledgements

A.K. is grateful for a stipend from the Erasmus-Mundus-Action-1-program (SINCHEM; FPA2013-0037).

Key words: Methanol • Homogeneous Catalysis • Mechanism • DFT • Hydrogen borrowing

- [1] A. Kaithal, M. Schmitz, M. Hölscher, W. Leitner, *ChemCatChem* **2019**, DOI: 10.1002/cctc.201900788.
- [2] a) P. T. Anastas, I. J. Levy, K. E. Parent, *Green Chemistry Education, Changing the Course of Chemistry* **2009**, 1011; b) P. T. Anastas, R. H. Crabtree, *Handbook of Green Chemistry, Volume 1., Green Catalysis, Homogeneous Catalysis* **2013**; c) S. Wesselbaum, T. vom Stein, J. Klankermayer, W. Leitner, *Angew. Chem. Int. Ed.* **2012**, *51*, 7499-7502; d) K. Natte, H. Neumann, M. Beller, R. V. Jagadeesh, *Angew. Chem. Int. Ed.* **2017**, *56*, 6384-6394; e) K. Oikawa, S. Itoh, H. Yano, H. Kawasaki, Y. Obora, *Chem Commun (Camb)* **2017**, 53, 1080-1083; f) S. M. A. H. Siddiki, A. S. Touchy, M. A. R. Jamil, T. Toyao, K.-i. Shimizu, *ACS Catal.* **2018**, *8*, 3091-3103; g) Q. Liu, G. Xu, Z. Wang, X. Liu, X. Wang, L. Dong, X. Mu, H. Liu, *ChemSusChem* **2017**, *10*, 4748-4755; h) Y. Li, H. Li, H. Junge, M. Beller, *Chem. Commun.* **2014**, *50*, 14991-14994.
- [3] A. Kaithal, P. v. Bonn, M. Hölscher, W. Leitner, *Angew. Chem. Int. Ed.* **2019**, DOI: 10.1002/anie.201909035.
- [4] a) M. Nielsen, E. Alberico, W. Baumann, H.-J. Drexler, H. Junge, S. Gladiali, M. Beller, *Nature* **2013**, *495*, 85; b) E. Alberico, A. J. J. Lennox, L. K. Vogt, H. Jiao, W. Baumann, H.-J. Drexler, M. Nielsen, A. Spannenberg, M. P. Checinski, H. Junge, M. Beller, *J. Am. Chem. Soc.* **2016**, *138*, 14890-14904; c) C. Gunanathan, D. Milstein, *Chem. Rev.* **2014**, *114*, 12024-12087; d) X. Yang, *ACS Catal.* **2013**, *3*, 2684-2688.
- [5] a) A. T. Nielsen, W. J. Houlihan, in *Organic Reactions*, **2011**, pp. 1-438; b) A. Balog, C. Harris, K. Savin, X.-G. Zhang, T.-C. Chou, S. J. Danishefsky, *Angew. Chem. Int. Ed.* **1998**, *37*, 2675-2678.
- [6] a) J. Neumann, C. Bornschein, H. Jiao, K. Junge, M. Beller, *Eur. J. Org. Chem.* **2015**, *2015*, 5944-5948; b) D. H. Nguyen, G. Raffa, Y. Morin, S. Dessel, F. Capet, V. Nardello-Rataj, F. Dumeignil, R. M. Gauvin, *Green Chemistry* **2017**, *19*, 5665-5673.
- [7] B. Chatterjee, C. Gunanathan, *Org. Lett.* **2015**, *17*, 4794-4797.
- [8] S. Kozuch, S. Shaik, *Acc. Chem. Res.* **2011**, *44*, 101-110.
- [9] B. Suchand, G. Satyanarayana, *Eur. J. Org. Chem.* **2017**, *2017*, 3886-3895.
- [10] A more detailed comparison between the experimental and the computed Gibbs free activation barrier can be obtained by conducting a thorough experimental kinetic analysis together with a detailed microkinetic modeling study.^[11] However, the challenges associated with the kinetic analysis in such a complex experimental system are significant, prompting us to refrain from performing such a study.
- [11] Recent leading references on microkinetic modeling and the challenges associated with combined computational/experimental analysis in mechanistic studies

which rely on computed data are: a) M. Besora, P. Vidossich, A. Lledós, G. Ujaque, F. Maseras, *J. Phys. Chem. A*, **2018**, *122*, 1392-1399; b) M. Besora, F. Maseras, *WIREs Comput. Mol. Sci.* **2018**, *8*, e1372; c) J. N. Harvey, F. Himo, F. Maseras, L. Perrin, *ACS Catal.* **2019**, *9*, 6803-6813.

WILEY-VCH

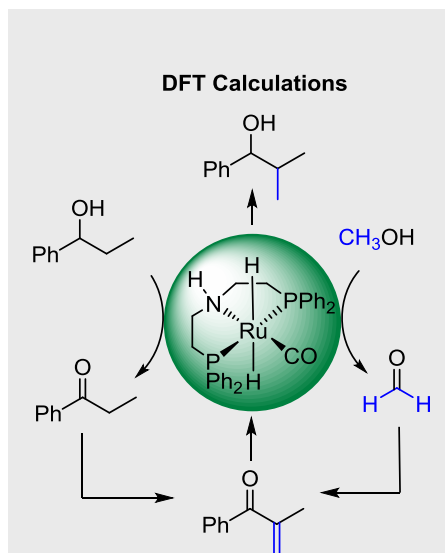
Accepted Manuscript

Entry for the Table of Contents (Please choose one layout)

Layout 1:

COMMUNICATION

Theoretical studies and experiments reveal the microscopic events in the methylation of alcohols with methanol in a ruthenium and base catalysed reaction with a complex reaction network.



Akash Kaithal, Marc Schmitz, Markus Hölscher,* Walter Leitner*

Page No. – Page No.

On the mechanism of the Ruthenium-catalyzed β -methylation of alcohols with methanol

Layout 2: